J. Fluid Mech. (1989), *vol.* 199, *pp.* 257–279
Printed in Great Britain

Onset of Rayleigh–Bénard convection in a rigid channel

By M. S. CHANA AND P. G. DANIELS
Department of Mathematics, The City University, Northampton Square, London, EC1V 0HB, UK

(Received 3 December 1987)

A two-dimensional Galerkin formulation of the three-dimensional Oberbeck–Boussinesq equations is used to describe the onset of convection in an infinite rigid horizontal channel uniformly heated from below. The dependence of the critical Rayleigh number on the channel aspect ratio is determined and results are compared with those of an idealized model studied by Davies-Jones (1970). Asymptotic results are derived for both narrow and wide channels, corresponding to limits of small and large aspect ratios respectively. In the latter case the main core flow, consisting of two-dimensional rolls with axes perpendicular to the vertical walls of the channel, can be represented by the solution of an amplitude equation. Close to the walls, however, the motion remains fully three-dimensional and a reversal of the vertical flow is associated with a local subdivision of each main roll into a pair of co-rotating rolls.

1. Introduction

Thermal convection is an important mechanism of heat and mass transfer in many geophysical, astrophysical and technological areas. There are an increasing number of applications in modern man-made environments such as energy storage systems, reactors and solar collectors where the flow is partly or completely confined. It is known from experimental work concerned with predicting the transition to turbulence in a fluid layer heated from below that the walls of the container have an important influence on the cell structure, even in layers of large lateral extent (Koschmieder 1966). It is therefore important, in gaining an understanding of the results of such experiments, to develop a theoretical treatment which takes full account of the lateral walls. Significant advances have been made in this area over the last twenty years. Davis (1967) used a Galerkin method to model the three-dimensional Boussinesq equations in a rectangular box and showed that the preferred mode of convection takes the form of horizontal rolls with axes aligned parallel to the shorter side of the box. Later Davies-Jones (1970) showed that the 'finite rolls' used in the Galerkin procedure (cells with two non-zero velocity components dependent on all three spatial coordinates) cannot be exact solutions of the linearized equations and boundary conditions, and developed an analytical model for the case of an infinite rectangular channel with stress-free horizontal boundaries where the full three-dimensional solution can be constructed. The results obtained from the solution of an eighth-order ordinary differential eigenvalue problem showed that the preferred mode closely resembles the finite-roll solutions of Davis. Further work on the rectangular box using an improved three-dimensional Galerkin simulation was reported by Catton (1970).

Nonlinear effects in rectangular containers of large horizontal planform were first considered by Segel (1969) and later by Brown & Stewartson (1977), who confirmed theoretically the preference for rolls parallel to the shorter side. At finite aspect ratios, simpler two-dimensional models where the rolls are aligned with axes parallel to the lateral walls (Drazin 1975) do not correspond to the preferred mode of convection established by Davies-Jones (1970) although the consideration of such models at large aspect ratios (Daniels 1978; Cross *et al.* 1983) has led to some progress in the understanding of how the lateral walls influence the wavelength selection process at finite amplitudes. Experiments by Buhler, Kirchartz & Oertel (1979) on Rayleigh–Bénard convection in long rectangular boxes have demonstrated how, at small Prandtl numbers, the wavelength of the convective rolls (which are aligned parallel to the two ends, consistent with Davis' numerical results) increases as the Rayleigh number is raised. A similar behaviour has been observed in shallow circular cylinders heated from below (Koschmieder & Pallas 1974). While numerical simulations for rectangular boxes (Buhler *et al.* 1979; Kessler 1987) are able to reproduce many of the observed features of the flow including the wavelength adjustment, a complete understanding requires a theoretical description of the adjustment mechanism. With this in mind, the most useful theoretical model of the long rectangular box appears to be one based on the infinite rectangular channel of Davies-Jones (1970) but with fully rigid bounding walls, necessitating a two-dimensional Galerkin representation of the cross-channel dependence but allowing an analytical description in terms of the third coordinate measured along the length of the channel. It is the latter dependence that corresponds to any adjustment in the wavelength of the roll pattern and it is anticipated that the influence of the distant endwalls of a realistic, three-dimensional long rigid box can be taken into account using the multiple-scaling and matching methods developed for the simpler two-dimensional models by Daniels (1977, 1978) and Cross *et al.* (1983).

The first requirement, then, is a description of the linearized solution of the three-dimensional Boussinesq equations at the onset of convection in an infinite rectangular channel with rigid walls, and this is the problem considered here. Unlike the Galerkin procedures used by Davis (1967), Catton (1970) and others, where three-dimensional solutions are constructed by superposing sets of finite-roll solutions in the two horizontal directions, here a Galerkin representation is required only for the two-dimensional cross-channel dependence. This allows trial functions to be constructed that take full account of the cross-channel horizontal velocity component, which would be set to zero in the corresponding finite-roll approximation. The governing equations and boundary conditions are stated in §2. The Galerkin formulation is described in §3 and results for the dependence of the critical Rayleigh number on the aspect ratio of the channel, $2a$ (width/height), are given. For $a > a_c$, where $\frac{1}{2} < a_c < 1$, it is found that the vertical velocity profile across the channel reverses sign near each sidewall. A re-examination of the idealized model with stress-free horizontal boundaries studied by Davies-Jones (1970) shows that the same phenomenon occurs there and streamline computations identify a subdivision of the main-cell circulation in the core into two separate curved cells near each sidewall. This behaviour is confirmed by an asymptotic description of the idealized flow for wide channels ($a \to \infty$) in §4.1. The flow domain can be formally divided into a main core zone where, to leading order, the circulation is two-dimensional and parallel to the channel walls, and sidewall regions where it remains fully three-dimensional. The description of the core solution involves the use of the linearized form of the amplitude equation first given by Segel (1969) and Newell & Whitehead (1969).

Asymptotic forms of the critical Rayleigh number and wavenumber for the idealized problem at small aspect ratios ($a \to 0$) are considered in §§4.2 and 4.3. Here the thermal conditions on the sidewalls are of primary significance and results are obtained for both conducting and insulating walls. In §§5 and 6 the various asymptotic results are extended to the case of the fully rigid channel. At large aspect ratios ($a \to \infty$) this involves the derivation of the linearized form of the appropriate amplitude equation. Boundary conditions obtained by matching with solutions near the sidewalls allow the corrections to the critical Rayleigh number and wavenumber of the corresponding infinite layer to be determined. At small aspect ratios ($a \to 0$) a different subdivision of the flow domain, into a main core region and end zones near the upper and lower boundaries, is required. Here the leading approximations to the critical Rayleigh number and wavenumber are found to coincide with those of the idealized problem. A brief discussion of the results is given in §7.

2. Governing equations

Fluid is contained in an infinite horizontal rectangular channel $|y| \leqslant a$, $|z| \leqslant \frac{1}{2}$, where x, y, z are coordinates non-dimensionalized with respect to the depth of the channel d, and with the x-axis along the centre of the channel. Steady linear motions in the Boussinesq approximation are governed by the non-dimensional equations

$$\frac{\partial u}{\partial x}+\frac{\partial v}{\partial y}+\frac{\partial w}{\partial z}=0, \tag{2.1}$$

$$\nabla^2 u-\frac{\partial p}{\partial x}=0, \tag{2.2}$$

$$\nabla^2 v-\frac{\partial p}{\partial y}=0, \tag{2.3}$$

$$\nabla^2 w+R\theta-\frac{\partial p}{\partial z}=0, \tag{2.4}$$

$$\nabla^2 \theta+w=0, \tag{2.5}$$

where θ and p are non-dimensional measures of the temperature θ^* and pressure p^* relative to the static, vertically stratified basic state:

$$\theta^* = \theta_0^* - \Delta\theta^* z + \Delta\theta^* \theta, \tag{2.6}$$

$$p^* = p_0^* - g\rho_0 \,\mathrm{d}z(1+\tfrac{1}{2}\alpha\,\Delta\theta^* z) + \rho_0 \kappa\nu\,\mathrm{d}^{-2} p. \tag{2.7}$$

Here $\theta_0^* \mp \frac{1}{2}\Delta\theta^*$ are the constant temperatures of the upper and lower surfaces of the channel, ρ_0 is the fluid density at the mean temperature θ_0^*, g is the acceleration due to gravity which acts in the negative-z direction and α, ν and κ are the coefficient of thermal expansion, kinematic viscosity and thermal diffusivity of the fluid respectively. The velocity components u, v, w are non-dimensionalized with respect to κ/d, and in (2.4) the Rayleigh number R is defined by

$$R = \alpha g\,\Delta\theta^* d^3/\kappa\nu. \tag{2.8}$$

For a channel with rigid, perfectly conducting walls the boundary conditions at $y = \pm a$ ($|z| \leqslant \frac{1}{2}$) and $z = \pm\frac{1}{2}$ ($|y| \leqslant a$) are

$$u = v = w = \theta = 0, \tag{2.9}$$

and since the primary interest is in applications to long totally enclosed boxes, the volume flux down the channel must be zero

$$\int_{-a}^{a}\int_{-\frac{1}{2}}^{\frac{1}{2}} u\,\mathrm{d}y\,\mathrm{d}z = 0, \tag{2.10}$$

thereby excluding from consideration pressure-driven flows of Poiseuille type, but not, in general, velocity and temperature fields that remain bounded as $|x| \to \infty$. The equations (2.1)–(2.5) are independent of the Prandtl number of the fluid and so the critical Rayleigh number for instability in the form of stationary convection depends only on the aspect ratio of the channel. A complementary numerical study of the problem with insulating sidewalls has been made by Luijkx & Platten (1981).

3. Galerkin formulation

Normal-mode solutions of (2.1)–(2.5) and (2.9) may be expressed in the form

$$(\theta, u, v, w, p) = \mathrm{e}^{\mathrm{i}qx}(\Theta, \mathrm{i}U, V, W, P)\,(y, z), \tag{3.1}$$

where q is a wavenumber for variations along the channel. Substitution into (2.1)–(2.5) gives

$$-qU + \frac{\partial V}{\partial y} + \frac{\partial W}{\partial z} = 0, \tag{3.2}$$

$$\bar{\nabla}^2 U - qP = 0, \tag{3.3}$$

$$\bar{\nabla}^2 V - \frac{\partial P}{\partial y} = 0, \tag{3.4}$$

$$\bar{\nabla}^2 W + R\Theta - \frac{\partial P}{\partial z} = 0, \tag{3.5}$$

$$\bar{\nabla}^2 \Theta + W = 0, \tag{3.6}$$

where

$$\bar{\nabla}^2 = \frac{\partial^2}{\partial y^2} + \frac{\partial^2}{\partial z^2} - q^2. \tag{3.7}$$

Elimination of P and U using the first two equations leads to the coupled system

$$\bar{\nabla}^2\left(\left(\frac{\partial^2}{\partial y^2} - q^2\right)V + \frac{\partial^2 W}{\partial y\,\partial z}\right) = 0, \tag{3.8}$$

$$\bar{\nabla}^2\left(\left(\frac{\partial^2}{\partial z^2} - q^2\right)W + \frac{\partial^2 V}{\partial y\,\partial z}\right) - Rq^2\Theta = 0, \tag{3.9}$$

$$\bar{\nabla}^2 \Theta + W = 0, \tag{3.10}$$

for V, W and Θ, to be solved subject to the boundary conditions

$$V = \frac{\partial V}{\partial y} = W = \Theta = 0 \quad \text{on } y = \pm a, \tag{3.11}$$

$$V = W = \frac{\partial W}{\partial z} = \Theta = 0 \quad \text{on } z = \pm\tfrac{1}{2}. \tag{3.12}$$

The flux condition (2.10) is then automatically satisfied, from integration of (3.2)

over the cross-section of the channel. The reduced two-dimensional system (3.8)–(3.12) provides a convenient formulation for application of the Galerkin method in which the solutions are expressed as

$$\Theta = \sum_{k=1}^{N} a_k \Theta_k(y,z), \quad W = \sum_{k=1}^{N} b_k W_k(y,z), \quad V = \sum_{k=1}^{N} c_k V_k(y,z), \tag{3.13}$$

with the trial functions taken to be

$$\left.\begin{aligned} \Theta_k &= \cos(2m-1)\frac{\pi y}{2a}\cos(2n-1)\pi z, \quad W_k = C_n(z)\cos(2m-1)\frac{\pi y}{2a} \\ V_k &= S_m\left(\frac{y}{2a}\right)\sin 2n\pi z \quad (m = 1,2,\ldots, \quad n = 1,2,\ldots). \end{aligned}\right\} \tag{3.14}$$

Here C_n and S_m are the beam functions defined by

$$C_n(z) = \frac{\cosh\lambda_n z}{\cosh\frac{1}{2}\lambda_n} - \frac{\cos\lambda_n z}{\cos\frac{1}{2}\lambda_n}, \quad S_m(\bar{y}) = \frac{\sinh\mu_m \bar{y}}{\sinh\frac{1}{2}\mu_m} - \frac{\sin\mu_m \bar{y}}{\sin\frac{1}{2}\mu_m}, \tag{3.15}$$

where λ_n and μ_m are the positive roots of the equations

$$\tanh\tfrac{1}{2}\lambda + \tan\tfrac{1}{2}\lambda = 0, \quad \coth\tfrac{1}{2}\mu - \cot\tfrac{1}{2}\mu = 0. \tag{3.16}$$

Their properties are discussed by Harris & Reid (1958). The functions (3.14) are chosen to satisfy the boundary conditions (3.11), (3.12) and to have the symmetries in y and z expected of the leading eigenmode. The summations in (3.13) for $k = 1,\ldots,$ N are taken over all integer combinations (m,n) following the ordering shown in table 1 below.

The forms (3.13) are substituted into the three equations (3.8)–(3.10) which are then multiplied by $V_{\bar{k}}$, $W_{\bar{k}}$ and $\Theta_{\bar{k}}$ ($\bar{k} = 1,2,\ldots,N$) respectively and integrated over the cross-section of the channel to obtain a set of $3N$ linear algebraic equations for the coefficients $a_k, b_k, c_k (k = 1,\ldots,N)$. These are

$$\sum_{k=1}^{N}\int_{-a}^{a}\int_{-\frac{1}{2}}^{\frac{1}{2}} V_{\bar{k}}\left[c_k\bar{\nabla}^2\left(\frac{\partial^2}{\partial y^2}-q^2\right)V_k + b_k\bar{\nabla}^2\frac{\partial^2 W_k}{\partial y\,\partial z}\right]dy\,dz = 0, \tag{3.17}$$

$$\sum_{k=1}^{N}\int_{-a}^{a}\int_{-\frac{1}{2}}^{\frac{1}{2}} W_{\bar{k}}\left[b_k\bar{\nabla}^2\left(\frac{\partial^2}{\partial z^2}-q^2\right)W_k + c_k\bar{\nabla}^2\frac{\partial^2 V_k}{\partial y\,\partial z} - Rq^2 a_k\Theta_k\right]dy\,dz = 0, \tag{3.18}$$

$$\sum_{k=1}^{N}\int_{-a}^{a}\int_{-\frac{1}{2}}^{\frac{1}{2}} \Theta_{\bar{k}}\left[a_k\bar{\nabla}^2\Theta_k + b_k W_k\right]dy\,dz = 0. \tag{3.19}$$

Orthogonality properties of the sinusoidal and beam functions in (3.14) imply that only certain terms make non-zero contributions to these equations. Thus if $(\bar{m},\bar{n})$ are the dual parameters associated with $\bar{k}$, the first term in (3.17) contributes only when $\bar{n} = n$, although the second always contributes. In (3.18) the first and third terms contribute only when $\bar{m} = m$ while the second always contributes. Finally, in (3.19) the first term only contributes when $\bar{k} = k$ ($\bar{m} = m$ and $\bar{n} = n$) and the second when $\bar{m} = m$. All of the integrals that do contribute can be evaluated analytically using results given by Reid & Harris (1958) and their values (see Appendix) form the non-zero elements of the $3N \times 3N$ coefficient matrix whose determinant must vanish in order that the system has a non-trivial solution for a_k, b_k, c_k ($k = 1,\ldots,N$). For a

given aspect ratio a the first zero of the determinant (corresponding to the lowest value of R) determines the location of the neutral curve for a stationary disturbance of wavenumber q. The zero was found using Newton's method to adjust the value of R at a given value of q, working to within a tolerance of six significant figures in the value of R. The minimum value of R as a function of q was located numerically for truncation levels up to $N = 10$, at which point a reasonable level of convergence was achieved, probably to within $\frac{1}{4}\%$ in both the critical wavenumber q_c and critical Rayleigh number R_c. A typical set of results for a square channel ($a = \frac{1}{2}$) is shown in table 1, and the corresponding neutral curves in figure 1. Further extensive calculations for the square channel by Daniels & Ong (1988) have shown that, for $N = 25$, $q_c = 3.3812$ and $R_c = 2944.3$, and higher modes of convection have also been calculated using the present method.

The critical Rayleigh number and wavenumber are shown as functions of the aspect ratio in figures 2 and 3, along with asymptotic results for small and large values of a discussed in §§5 and 6. It is interesting to note that for aspect ratios $a \gtrsim 0.7$ the critical wavenumber q_c falls below the value 3.117 for the infinite layer, just as it does in the corresponding idealized problem with stress-free horizontal boundaries studied by Davies-Jones (1970). This behaviour appears to be related to the three-dimensional nature of the flow near the sidewalls which is discussed in detail in §4. Velocity and temperature profiles in the cross-section of the channel (figures 4 and 5) indicate an interesting behaviour for large aspect ratios (for example $a = 1$, figure 5) in which the vertical velocity near the sidewall reverses sign. Although this behaviour was not reported by Davies-Jones (1970) a closer examination of the stress-free model demonstrates that it also occurs there, suggesting that it is associated with the rigidity of the sidewall.

In the idealized model the boundary conditions (2.9) at $z = \pm\frac{1}{2}$ are replaced by

$$w = \frac{\partial u}{\partial z} = \frac{\partial v}{\partial z} = \theta = 0 \quad (z = \pm\tfrac{1}{2}), \tag{3.20}$$

allowing the leading eigensolutions (3.13) to be expressed in the form

$$\Theta = \bar{\Theta}(y)\sin\pi(z+\tfrac{1}{2}), \quad W = \bar{W}(y)\sin\pi(z+\tfrac{1}{2}), \quad V = \bar{V}(y)\cos\pi(z+\tfrac{1}{2}), \tag{3.21}$$

with $U = \bar{U}(y)\cos\pi(z+\frac{1}{2})$. Substitution into (3.8)–(3.10) and elimination of $\bar{W}$ gives

$$\left\{\left(\frac{\mathrm{d}^2}{\mathrm{d}y^2}-\delta^2\right)^3 - R\left(\frac{\mathrm{d}^2}{\mathrm{d}y^2}-q^2\right)\right\}\bar{\Theta} = 0,$$

$$\left(\frac{\mathrm{d}^2}{\mathrm{d}y^2}-\delta^2\right)\bar{V} = \pi^{-1}\left\{\left(\frac{\mathrm{d}^2}{\mathrm{d}y^2}-\delta^2\right)^2 - R\right\}\frac{\mathrm{d}\bar{\Theta}}{\mathrm{d}y}, \tag{3.22}$$

with boundary conditions

$$\bar{\Theta} = \left(\frac{\mathrm{d}^2}{\mathrm{d}y^2}-\delta^2\right)\bar{\Theta} = \bar{V} = \frac{\mathrm{d}\bar{V}}{\mathrm{d}y} = 0 \quad (y = \pm a), \tag{3.23}$$

where $\delta^2 = q^2+\pi^2$. The leading mode, for which $\bar{\Theta}$ is even and $\bar{V}$ is odd, can be expressed as

$$\bar{\Theta} = \sum_{j=1}^{3} d_j \cosh r_j y, \quad \bar{V} = \sum_{j=1}^{3} \mathrm{d}_j \beta_j \sinh r_j y + \mathrm{d}_4 \sinh \delta y, \tag{3.24}$$

where

$$\beta_j = R\pi r_j / s_j^2 \tag{3.25}$$

m	n	N	q_c	R_c	a_1	b_1	a_2	b_2	c_2
1	1	1	3.4966	3115.61	0.6441	14.76	—	—	—
1	2	2	3.5126	3056.47	0.6633	15.19	0.0263	0.4080	−0.2437
2	1	3	3.4036	2972.99	0.3447	7.712	0.0136	0.1934	−0.1616
2	2	4	3.4031	2971.02	0.3520	7.873	0.0137	0.2130	−0.2307
1	3	5	3.4015	2964.28	0.3554	7.943	0.0136	0.2275	−0.2637
2	3	6	3.4016	2964.09	0.3553	7.941	0.0136	0.2275	−0.2626
3	1	7	3.3881	2952.29	0.3440	7.666	0.0131	0.2181	−0.2567
3	2	8	3.3881	2952.02	0.3448	7.682	0.0131	0.2218	−0.2616
3	3	9	3.3881	2951.98	0.3447	7.680	0.0131	0.2218	−0.2617
1	4	10	3.3871	2950.03	0.3464	7.715	0.0131	0.2265	−0.2663

TABLE 1. Convergence of the Galerkin scheme for $a = \frac{1}{2}$; the coefficients are normalized with $c_1 = 1$

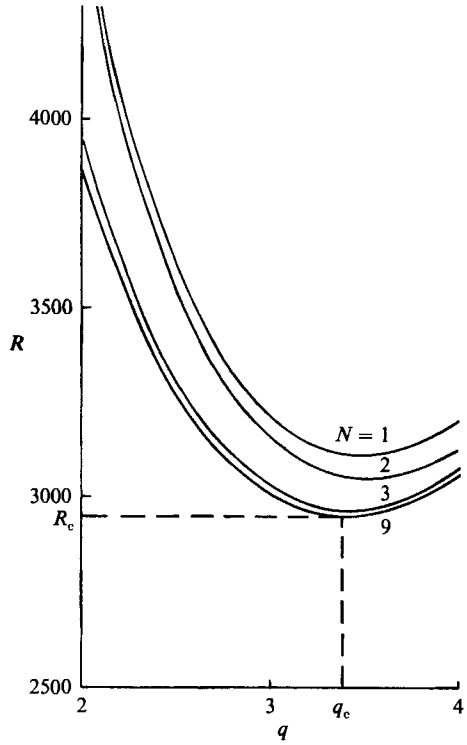

FIGURE 1. Convergence of the neutral curve with truncation level N for $a = \frac{1}{2}$.

and $r_j^2 = s_j + \delta^2$, where $s_j (j = 1, 2, 3)$ are the three roots of

$$s^3 - Rs - \pi^2 R = 0, \tag{3.26}$$

which, for the range of interest, $R > \frac{27}{4}\pi^4$, are real and distinct. From (3.23),

$$\begin{bmatrix} 1 & 1 & 1 & 0 \\ s_1 & s_2 & s_3 & 0 \\ \beta_1 r_1 & \beta_2 r_2 & \beta_3 r_3 & \delta \\ \beta_1 \tanh r_1 a & \beta_2 \tanh r_2 a & \beta_3 \tanh r_3 a & \tanh \delta a \end{bmatrix} \begin{bmatrix} \mathrm{d}_1 \cosh r_1 a \\ \mathrm{d}_2 \cosh r_2 a \\ \mathrm{d}_3 \cosh r_3 a \\ \mathrm{d}_4 \cosh \delta a \end{bmatrix} = \begin{bmatrix} 0 \\ 0 \\ 0 \\ 0 \end{bmatrix} \tag{3.27}$$

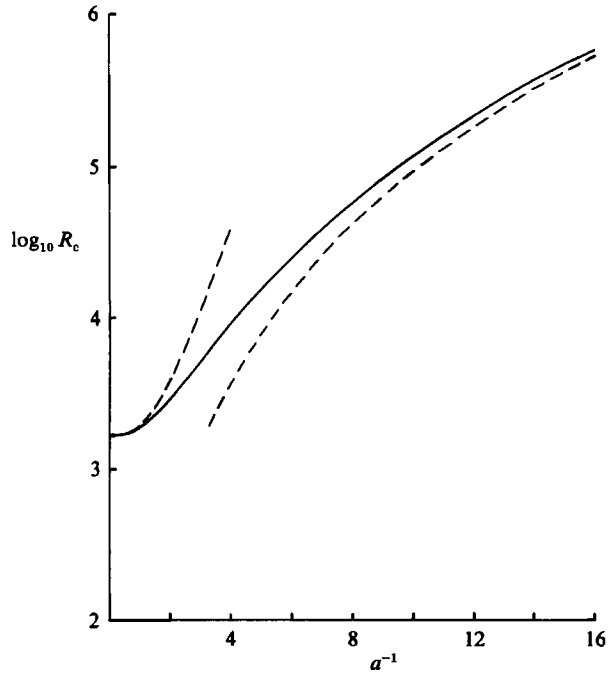

FIGURE 2. Dependence of the critical Rayleigh number on aspect ratio for a rigid channel with conducting sidewalls. Relevant asymptotic results (4.25) and (5.23) for small and large values of a are shown by dashes.

and the neutral curve is determined by locating the zeros of the determinant of the coefficient matrix, a task that is simplified by the fact that for $R > \frac{27}{4}\pi^4$ the determinant is either purely real or purely imaginary. Results for the neutral curves agreed with those given by Davies-Jones (1970), whose analysis did not explicitly incorporate the symmetry of the solution. Profiles of $\bar{\Theta}$, $\bar{W}$ and $\bar{V}$ (figure 6) exhibited the same tendencies as those of the fully rigid problem, with a region of reversed vertical flow near the sidewalls for aspect ratios $a > a_c$ where $\frac{1}{2} < a_c < 1$; velocity contours (figure 7) clearly show the sidewall region although those given earlier by Davies-Jones are not sufficiently detailed to do so. The same behaviour occurs if the sidewalls are adiabatic, and further results for this case are reported by Chana (1986). The behaviour can best be interpreted physically by plotting the three-dimensional streamlines of the flow. On taking the real parts of (3.1) and using (3.21) the streamline passing through an arbitrary point (x_0, y_0, z_0) is found to be given by

$$\left.\begin{aligned} x &= q^{-1}\sin^{-1}\left[\sin(qx_0)\exp\left\{-q\int_{y_0}^{y}\frac{\bar{U}}{\bar{V}}\,\mathrm{d}y\right\}\right], \\ z+\tfrac{1}{2} &= \pi^{-1}\sin^{-1}\left[\sin(\pi[z_0+\tfrac{1}{2}])\exp\left\{\pi\int_{y_0}^{y}\frac{\bar{W}}{\bar{V}}\,\mathrm{d}y\right\}\right]. \end{aligned}\right\} \tag{3.28}$$

Figures 8 and 9 show typical members of this family of curves for two values of a. At the smaller aspect ratio (figure 8), particles move in closed loops distorted only slightly by the cross-channel velocity component v, so that the motion closely approximates a finite-roll pattern with roll axis perpendicular to the sidewalls of the channel. At the larger aspect ratio (figure 9) a similar flow occurs in the centre of the

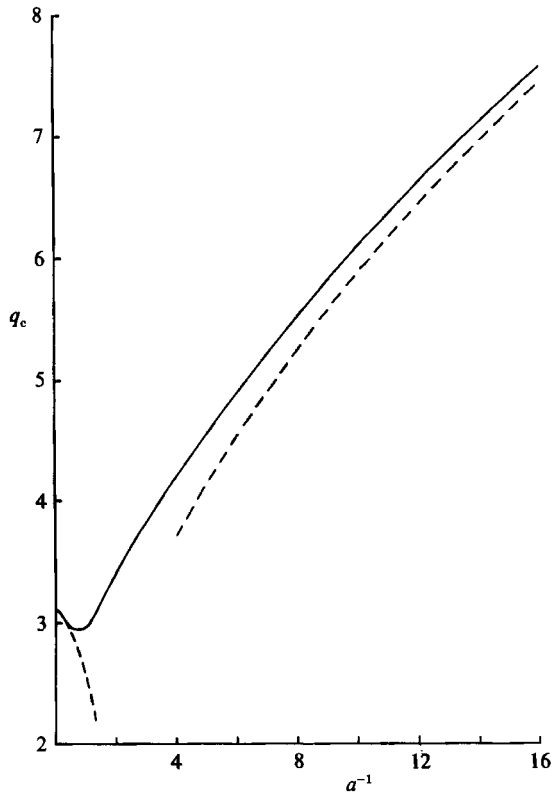

FIGURE 3. Dependence of the critical wavenumber on aspect ratio for a rigid channel with conducting sidewalls. Relevant asymptotic results (4.25) and (5.23) for small and large values of a are shown by dashes.

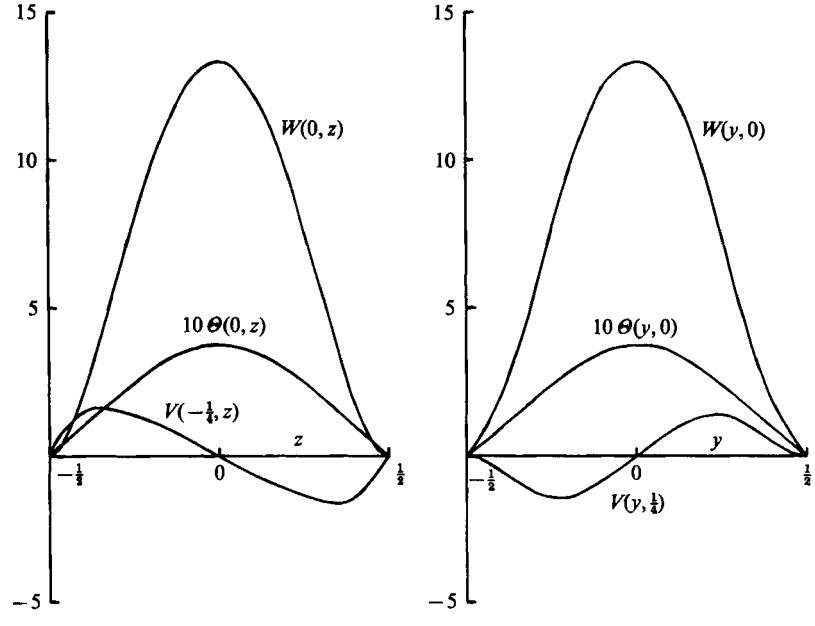

FIGURE 4. Velocity and temperature profiles at the onset of convection ($R_c = 2950$, $q_c = 3.39$) in a rigid channel with conducting sidewalls and $a = \frac{1}{2}$.

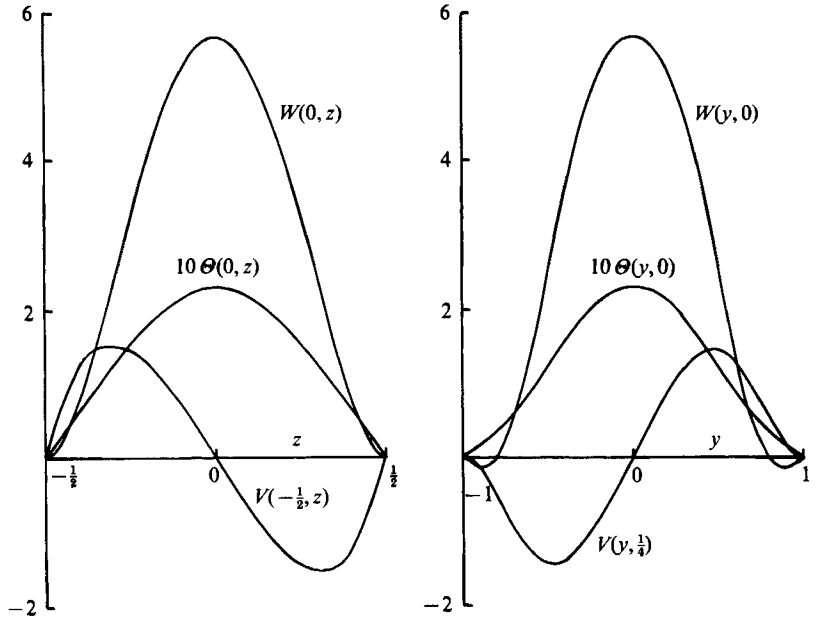

FIGURE 5. Velocity and temperature profiles at the onset of convection ($R_c = 1874$, $q_c = 2.95$) in a rigid channel with conducting sidewalls and $a = 1$.

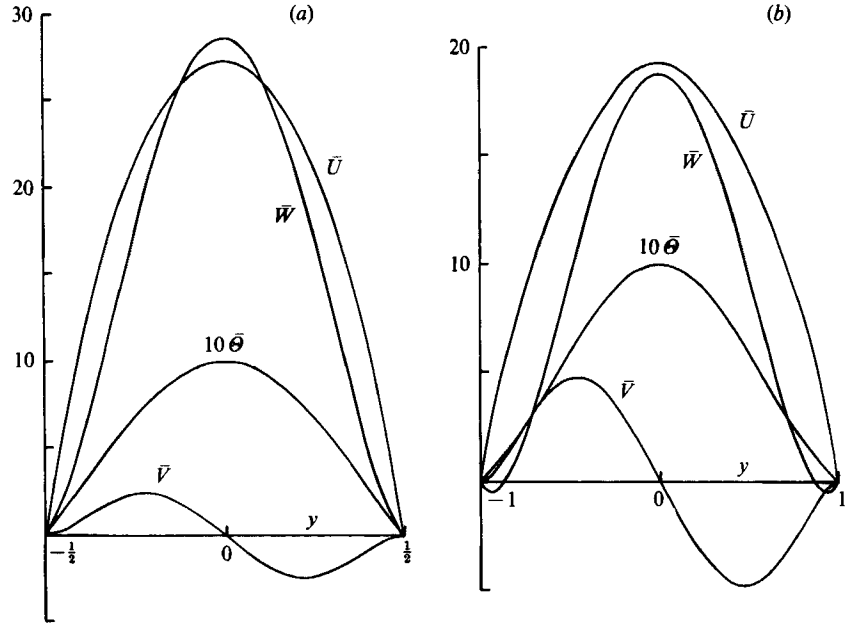

FIGURE 6. Velocity and temperature profiles at the onset of convection for the idealized channel with conducting sidewalls: (*a*) $a = \frac{1}{2}$ ($R_c = 1654.74$, $q_c = 2.7021$), (*b*) $a = 1$ ($R_c = 827.57$, $q_c = 2.2315$).

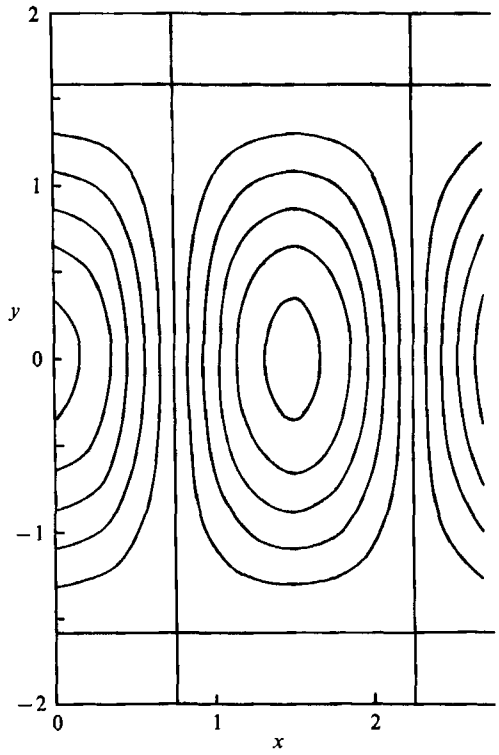

FIGURE 7. Horizontal planform of the cells at the onset of convection in the idealized channel with conducting sidewalls and $a = 2$, showing vertical velocity contours at $z = 0$.

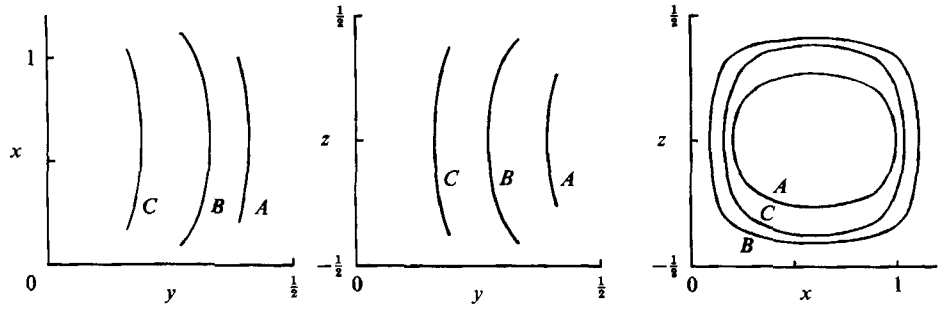

FIGURE 8. Projections of three streamlines A, B, C in the coordinate planes at the onset of convection for the idealized channel with conducting sidewalls and $a = \frac{1}{2}$.

channel but near the sidewalls the reversal of the vertical velocity is seen to be associated with a splitting of each main roll into a pair of curved corotating rolls. The flow must be three-dimensional since finite-roll solutions are not exact solutions of the governing equations in the presence of rigid sidewalls. When the walls are sufficiently far apart, the local bending of rolls appears to necessitate the splitting of the main roll. Physically, this may be the only way in which the fluid motion can retain something close to its characteristic critical wavelength near the sidewalls of the channel.

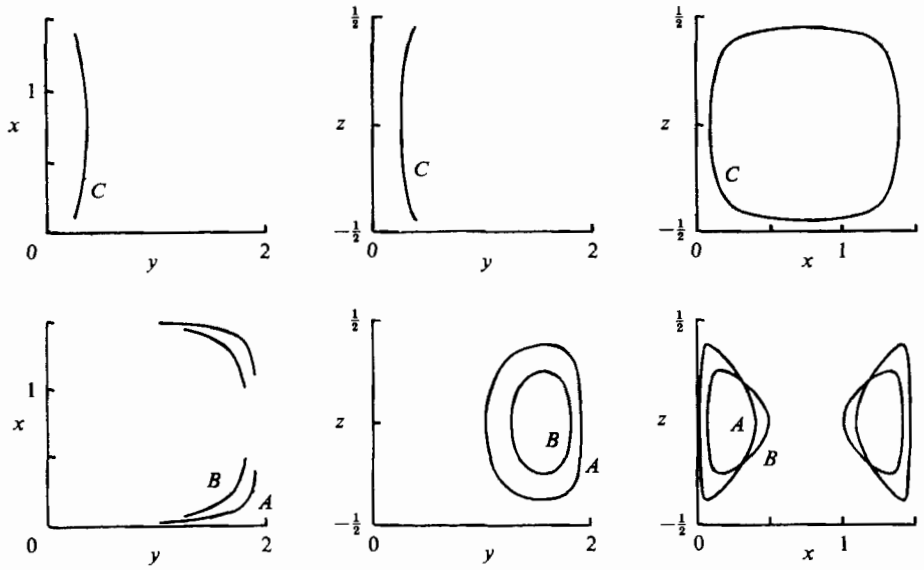

FIGURE 9. Projections of three streamlines A, B, C in the coordinate planes at the onset of convection for the idealized channel with conducting sidewalls and $a = 2$.

4. Asymptotic results for the idealized problem

In this section some asymptotic results for the problem studied by Davies-Jones (1970) are derived.

4.1. $a \to \infty$

The critical Rayleigh number approaches the value $\frac{27}{4}\pi^4$ associated with an infinite horizontal layer and numerical results suggest that locally the neutral curve is defined by

$$R \sim \tfrac{27}{4}\pi^4 + a^{-4}\bar{R}^2, \quad q^2 \sim \tfrac{1}{2}\pi^2 - a^{-2}\bar{q}, \tag{4.1}$$

where $\bar{R}$ and $\bar{q}$ remain finite as $a \to \infty$. It follows from (3.26) that

$$r_1 \sim \frac{3\pi}{\sqrt{2}}\left(1 - \frac{\bar{q}}{9\pi^2 a^2}\right), \quad r_2 \sim \mathrm{i}\omega_+/a, \quad r_3 \sim \omega_-/a \quad (a \to \infty), \tag{4.2}$$

where

$$\omega_\pm = (\tfrac{1}{3}\bar{R} \pm \bar{q})^{\frac{1}{2}} \tag{4.3}$$

and the leading contributions to the coefficient matrix in (3.27) are

$$\begin{bmatrix} 1 & 1 & 1 & 0 \\ 3\pi^2 & -\frac{3}{2}\pi^2 & -\frac{3}{2}\pi^2 & 0 \\ \frac{27}{8}\pi^3 & -3\pi\omega_+^2/a^2 & 3\pi\omega_-^2/a^2 & \sqrt{\frac{3}{2}}\pi \\ 9\pi^2/4\sqrt{2} & -3\pi a^{-1}\omega_+ \tan\omega_+ & 3\pi a^{-1}\omega_- \tanh\omega_- & 1 \end{bmatrix}, \tag{4.4}$$

where terms of relative order a^{-2} are neglected. The leading contributions to the determinant of (4.4) cancel but the order a^{-1} terms balance only if

$$\omega_+ \tan\omega_+ + \omega_- \tanh\omega_- = 0. \tag{4.5}$$

The lowest solution branch for $\bar{R}$ defines the neutral curve as a function of $\bar{q}$ and the

critical Rayleigh number is determined by the additional condition $\mathrm{d}\bar{R}^2/\mathrm{d}\bar{q} = 0$ from which it is found that $\bar{R} = \bar{R}_c = 13.905$ and $\bar{q} = \bar{q}_c = 3.1959$. Thus

$$R_c \sim \tfrac{27}{4}\pi^4 + 193.36a^{-4}, \quad q_c \sim \frac{\pi}{\sqrt{2}} - 0.719\,33a^{-2} \quad \text{as } a \to \infty. \tag{4.6}$$

The same results are also valid for insulating sidewalls and table 2 indicates a favourable comparison with numerical solutions obtained from both (3.27) and the corresponding adiabatic system.

The method of matched asymptotic expansions provides an alternative means of obtaining (4.6). The flow domain is subdivided into a core region $|Y| < 1$, where $Y = y/a$, and sidewall regions where $y \pm a = O(1)$. In the core the slow spatial variation can be represented by a temperature field

$$\theta \sim \mathrm{e}^{\frac{1}{\sqrt{2}}\pi z} A(X, Y) \sin \pi(z + \tfrac{1}{2}), \tag{4.7}$$

where the scaled coordinate $X = x/a^2$ accounts for wavelength adjustments in the neighbourhood of the critical value $\sqrt{2}$. Then if R is defined by (4.1) the linearized versions of the amplitude expansions of Newell & Whitehead (1969) and Segel (1969) imply that the amplitude function A satisfies

$$\left(\frac{\partial^2}{\partial Y^2} + \mathrm{i}\sqrt{2}\,\pi \frac{\partial}{\partial X}\right)^2 A - \tfrac{1}{9}\bar{R}^2 A = 0. \tag{4.8}$$

Furthermore, Brown & Stewartson (1977) demonstrate that the appropriate boundary conditions at $Y = \pm 1$ are

$$A = \frac{\partial A}{\partial Y} = 0. \tag{4.9}$$

The solution of (4.8) is expressed in the form $A = \mathrm{e}^{\frac{-\mathrm{i}\bar{q}X}{\sqrt{2}\pi}} \bar{A}(Y)$ so that $\bar{q}$ is equivalent to the constant defined in (4.1) and it follows that the leading even mode is

$$\bar{A} = \gamma \cos \omega_+ Y + (1 - \gamma) \cosh \omega_- Y, \tag{4.10}$$

where $\omega_\pm$ are defined by (4.3). This exists, subject to (4.9) provided that $\bar{q}$ and $\bar{R}$ are related by (4.5) and $\gamma^{-1} = 1 - \operatorname{sech} \omega_- \cos \omega_+$. The solution (4.10) is normalized such that $\bar{A} = 1$ at $Y = 0$.

The form (4.7) is inappropriate near each sidewall where there must be an adjustment to the full boundary conditions, which, in the conducting case, are given by (2.9). The solution is fully three-dimensional and is generated by the quadratic dependence of A as $|Y \pm 1| \to 0$. Thus it is expected that in the region where $\tilde{y} = y + a = O(1)$,

$$(\bar{\Theta}, \bar{U}, \bar{V}, \bar{W}) \sim a^{-2}(\tilde{\theta}, \tilde{u}, \tilde{v}, \tilde{w}), \tag{4.11}$$

and, since $R \approx \frac{27}{4}\pi^4$, substitution into (3.22) gives the coupled system

$$\left.\begin{aligned} \frac{\mathrm{d}^4}{\mathrm{d}\tilde{y}^4}\left(\frac{\mathrm{d}^2}{\mathrm{d}\tilde{y}^2} - \frac{9\pi^2}{2}\right)\tilde{\theta} &= 0, \\ \left(\frac{\mathrm{d}^2}{\mathrm{d}\tilde{y}^2} - \frac{3\pi^2}{2}\right)\tilde{v} &= \pi^{-1}\left(\frac{\mathrm{d}^4}{\mathrm{d}\tilde{y}^4} - 3\pi^2 \frac{\mathrm{d}^2}{\mathrm{d}\tilde{y}^2} - \frac{9\pi^4}{2}\right)\frac{\mathrm{d}\tilde{\theta}}{\mathrm{d}\tilde{y}}, \end{aligned}\right\} \tag{4.12}$$

to be solved subject to the boundary conditions

$$\tilde{\theta} = \frac{\mathrm{d}^2\tilde{\theta}}{\mathrm{d}\tilde{y}^2} = \tilde{v} = \frac{\mathrm{d}\tilde{v}}{\mathrm{d}\tilde{y}} = 0 \quad \text{on} \quad \tilde{y} = 0. \tag{4.13}$$

	Conducting sidewalls		Insulating sidewalls		Asymptotic formulae (4.6)	
a	q_c	R_c	q_c	R_c	q_c	R_c
1	2.2315	827.57	2.2680	799.44	1.5021	850.87
2	2.0977	673.60	2.1013	673.57	2.0416	669.60
3	2.1460	660.58	2.1449	660.58	2.1415	659.90
4	2.1760	658.44	2.1756	658.43	2.1765	658.27
5	2.1918	657.88	2.1917	657.88	2.1925	657.82

TABLE 2. Comparison of numerical results for R_c and q_c with the asymptotic formulae (4.6) for large aspect ratios

The general solution of (4.12) that avoids exponential growth as $\tilde{y} \to \infty$ is

$$\tilde{\theta} = \tilde{a}_0 + \tilde{a}_1 \tilde{y} + \tilde{a}_2 \tilde{y}^2 + \tilde{a}_3 \tilde{y}^3 + \tilde{a}_4 \mathrm{e}^{-\frac{3\pi}{\sqrt{2}}\tilde{y}}, \tag{4.14}$$

$$\tilde{v} = 3\pi\tilde{a}_1 + 6\pi\tilde{a}_2 \tilde{y} + \frac{3\tilde{a}_3(3\pi^2\tilde{y}^2+8)}{\pi} - \frac{9\pi^2\tilde{a}_4 \mathrm{e}^{-\frac{3\pi}{\sqrt{2}}\tilde{y}}}{4\sqrt{2}} + \tilde{a}_5 \mathrm{e}^{-\sqrt{\frac{3}{2}}\pi\tilde{y}}. \tag{4.15}$$

Matching with the core solution as $\tilde{y} \to \infty$ requires that

$$\tilde{a}_3 = 0, \quad \tilde{a}_2 = \frac{1}{2}\frac{\mathrm{d}^2\bar{A}}{\mathrm{d}Y^2}(-1) \tag{4.16}$$

and then from (4.13)

$$\tilde{a}_0 = -\tilde{a}_4 = 4\tilde{a}_2/9\pi^2, \quad \tilde{a}_1 = -(1+3\sqrt{3})\,\tilde{a}_2/3\sqrt{2}\pi, \quad \tilde{a}_5 = 3\sqrt{3}\,\tilde{a}_2/\sqrt{2}. \tag{4.17}$$

In the core the vertical velocity corresponding to (4.7) is given by

$$\bar{W} \sim \tfrac{3}{2}\pi^2\bar{A}(Y), \tag{4.18}$$

whereas in the sidewall region it is given by

$$\bar{W} \sim \frac{1}{2a^2}\frac{\mathrm{d}^2\bar{A}}{\mathrm{d}Y^2}(-1)\left\{\tfrac{4}{3}(\mathrm{e}^{-\frac{3\pi}{\sqrt{2}}\tilde{y}}-1) - \frac{\pi(1+3\sqrt{3})\,\tilde{y}}{2\sqrt{2}} + \tfrac{3}{2}\pi^2\tilde{y}^2\right\}. \tag{4.19}$$

This shows explicitly the region of reversed flow near $\tilde{y} = 0$. In fact the temperature profile (4.14) also reverses near $\tilde{y} = 0$; this trend is evident in figure 6(*b*) where $a = 1$, and the behaviour was confirmed by a computation at a higher aspect ratio, $a = 5$. Table 3 shows a comparison of the asymptotic formulae (4.14), (4.19) with numerical results for $a = 5$ based on the equivalent normalization $\bar{\Theta}(0) = 1$. Similar formulae for adiabatic walls also agree well with numerical results (Chana 1986).

4.2. $a \to 0$: *conducting sidewalls*

Numerical results and a 'finite-roll' approximation due to Davies-Jones (1970) suggest that for small aspect ratios and conducting sidewalls the neutral curve is approximated by

$$R \sim \frac{R_1}{a^4} + \frac{R_2}{a^3}, \quad q^2 \sim \frac{q_1}{a} + q_2, \tag{4.20}$$

where R_1, R_2, q_1 and q_2 are finite as $a \to 0$. Then from (3.26)

$$r_1 \sim R_1^{\frac{1}{4}}(a^{-1} + \tfrac{1}{2}[q_1 + \tfrac{1}{2}R_2 R_1^{-\frac{1}{2}}]R_1^{-\frac{1}{2}}), \quad r_2 \sim \mathrm{i}R_1^{\frac{1}{4}}(a^{-1} - \tfrac{1}{2}[q_1 - \tfrac{1}{2}R_2 R_1^{-\frac{1}{2}}]R_1^{-\frac{1}{2}}), \quad r_3 \sim (q_1/a)^{\frac{1}{2}} \tag{4.21}$$

Y	$\bar{W}$	$a^{-2}\tilde{w}$	$\bar{\Theta}$	$a^{-2}\tilde{\theta}$
−5	0	0	0	0
−4.875	−0.161	−0.159	−0.0013	−0.0020
−4.75	−0.207	−0.216	−0.0005	−0.0020
−4.625	−0.170	−0.199	0.0034	0.0009
−4.5	−0.066	−0.118	0.0170	0.0070
−4.375	0.097	0.019	0.0215	0.0166

Table 3. Comparison of numerical results for the temperature and vertical velocity near the sidewalls with the asymptotic results (4.14), (4.19), for $a = 5$

and the condition for a non-trivial solution of (3.27) reduces to

$$(s_2 - s_1)\, D - \mathrm{i}\pi q_1^{\frac{1}{2}} R_1^{\frac{3}{4}} a^{-\frac{7}{2}} \tanh r_2 a = O(a^{-\frac{7}{2}}), \tag{4.22}$$

where $D = \beta_3(r_3 \tanh \delta a - \delta \tanh r_3 a)$. Since $D \sim -R_1 q_1^{\frac{3}{2}}/3\pi a^{\frac{5}{2}}$ as $a \to 0$, it follows from (4.22) that

$$2q_1 R_1^{\frac{3}{4}}/3\pi^2 a + \tan\left[R_1^{\frac{1}{4}} - \tfrac{1}{2}(q_1 - \tfrac{1}{2}R_2 R_1^{-\frac{1}{2}})\, R_1^{-\frac{1}{4}} a\right] = O(1), \tag{4.23}$$

and this is only possible if $R_1 = m^4\pi^4/16$ $(m = 1, 3, 5, \ldots)$ and

$$R_2 = \tfrac{1}{2}\pi^2 q_1 (m^2 + 12 q_1^{-2}). \tag{4.24}$$

The leading mode corresponds to $m = 1$ and the additional condition $\mathrm{d}R_2/\mathrm{d}q_1 = 0$ determines the critical values $R_{2c} = 2\sqrt{3}\pi^2$ and $q_{1c} = 2\sqrt{3}$ associated with the minimum point of the neutral curve. Thus

$$R_c \sim \frac{\pi^4}{16a^4} + \frac{2\sqrt{3}\pi^2}{a^3}, \quad q_c \sim (2\sqrt{3}/a)^{\frac{1}{2}} \quad \text{as} \quad a \to 0. \tag{4.25}$$

The closeness of the sidewalls severely restricts the instability leading to the large value of R_c. Although the wavelength is small compared with the height of the channel it is large compared with the width.

4.3. $a \to 0$: *insulating sidewalls*

Here

$$u = v = w = \frac{\partial \theta}{\partial y} = 0 \quad \text{on} \quad y = \pm a \tag{4.26}$$

and the non-zero elements of the first row of the matrix in (3.27) are replaced by $r_i \tanh r_i a$ $(i = 1, 2, 3)$. If the same scalings (4.20) are assumed the result (4.22) is replaced by

$$a^{-3} R_1^{\frac{3}{4}} (\tan R_1^{\frac{1}{4}} - \tanh R_1^{\frac{1}{4}})\, D = O(a^{-\frac{7}{2}} \tan R_1^{\frac{1}{4}}) \tag{4.27}$$

and so $\tan R_1^{\frac{1}{4}} - \tanh R_1^{\frac{1}{4}} = 0$; the solutions $R_1 = R_1^{(m)}$ $(m = 1, 2, \ldots)$ define a family of horizontal modes, but here $R_1^{(1)} = 0$ indicating that the leading one is actually associated with different scalings of R and q. The numerical results suggest that for this mode

$$R \sim \frac{\bar{R}_1}{a^2} + \frac{\bar{R}_2}{a}, \quad q^2 \sim \bar{q}_1 + a\bar{q}_2, \tag{4.28}$$

with $\bar{R}_1, \bar{R}_2, \bar{q}_1$ and $\bar{q}_2$ finite as $a \to 0$, so that

$$\left.\begin{aligned} r_1 &\sim a^{-\frac{1}{2}} \bar{R}_1^{\frac{1}{4}} (1 + \tfrac{1}{2}[\bar{R}_2 \bar{R}_1^{-\frac{1}{2}} + \bar{q}_1 + \tfrac{3}{2}\pi^2]\, \bar{R}_1^{-\frac{1}{4}} a), \\ r_2 &\sim \mathrm{i} a^{-\frac{1}{2}} \bar{R}_1^{\frac{1}{4}} (1 + \tfrac{1}{2}[\bar{R}_2 \bar{R}_1^{-\frac{1}{2}} - \bar{q}_1 - \tfrac{3}{2}\pi^2]\, \bar{R}_1^{-\frac{1}{4}} a), \quad r_3 \sim \bar{q}_1^{\frac{1}{2}}. \end{aligned}\right\} \tag{4.29}$$

	Conducting sidewalls				Insulating sidewalls			
	Numerical		Asymptotic (4.25)		Numerical		Asymptotic (4.32)	
a	q_c	R_c	q_c	R_c	q_c	R_c	q_c	R_c
0.5	2.7021	1654.7	2.6322	370.92	2.4962	1277.6	3.1416	473.74
0.2	4.0223	12251	4.1618	8078.7	2.8542	3799.4	3.1416	2960.9
0.1	5.7281	10843×10	5.8857	95070	3.0407	12718	3.1416	11844
0.05	8.1904	12955×10^2	8.3236	12476×10^2	3.1133	48260	3.1416	47374

TABLE 4. Comparison of numerical results for R_c and q_c with the asymptotic formulae (4.25) and (4.32) for small aspect ratios

The condition for a non-trivial solution now reduces to

$$\tfrac{2}{3}\pi(\bar{q}_1+\pi^2)^{\frac{3}{4}}\bar{R}_1^{\frac{3}{4}}a+\bar{D}=0, \tag{4.30}$$

where $\bar{D}=(r_1 s_2\tanh r_1 a-r_2 s_1\tanh r_2 a)D$ and in this case $D\sim-(\bar{q}_1+\pi^2)^{\frac{1}{4}}\bar{q}_1\bar{R}_1 a/3\pi$ as $a\sim0$. Then $\bar{D}$ is also of order a and the balance of terms in (4.30) yields

$$\bar{R}_1=3\bar{q}_1^{-1}(\pi^2+\bar{q}_1)^2. \tag{4.31}$$

The critical parameter values determined by the condition $\mathrm{d}\bar{R}_1/\mathrm{d}\bar{q}_1=0$ are $\bar{R}_{1c}=12\pi^2$ and $\bar{q}_{1c}=\pi^2$, giving

$$R_c\sim12\pi^2a^{-2},\quad q_c\sim\pi\quad\text{as}\quad a\to0. \tag{4.32}$$

Thus the critical Rayleigh number is significantly lower than in the conducting case, and the wavelength significantly higher, consistent with the numerical calculations of Davies-Jones (1970). In fact it is seen that for insulating sidewalls the critical wavelength in a narrow channel is independent of aspect ratio and numerically equal to the depth of the channel, so that the thin rolls occupy square cross-sections parallel to the plane of the sidewalls, equivalent to a Hele-Shaw approximation to the motion.

The formulae (4.25) and (4.32) are compared with numerical results in table 4.

5. Asymptotic results for the rigid channel: $a\to\infty$

In the absence of a matrix form equivalent to (3.27) it is necessary to adopt the alternative approach described in §4.1. Thus it is assumed that

$$R\sim R_0+a^{-4}\bar{R}^2,\quad q^2\sim q_0^2-a^{-2}\bar{q}\quad\text{as}\quad a\to\infty, \tag{5.1}$$

where $R_0=1707.76$ and $q_0=3.117$ are the critical Rayleigh number and wavenumber for the infinite layer with rigid horizontal boundaries, and an amplitude equation equivalent to (4.8) is sought in order to describe the core motion where $|Y|<1$. A simple method of deriving this equation is to eliminate V and W in (3.8)–(3.10), (3.12) giving the following sixth order system for Θ:

$$\left.\begin{aligned}&\left(\bar{\nabla}^6-R\left[\frac{\partial^2}{\partial y^2}-q^2\right]\right)\Theta=0;\\ &\Theta=\frac{\partial^2\Theta}{\partial z^2}=\bar{\nabla}^2\frac{\partial\Theta}{\partial z}=0\quad(z=\pm\tfrac{1}{2}).\end{aligned}\right\} \tag{5.2}$$

The cross-channel core scaling and the correction to q_0^2 in (5.1) combine as a single operator

$$\mathrm{L} = \frac{\partial^2}{\partial Y^2} + \bar{q}, \tag{5.3}$$

so that

$$\left.\begin{aligned} &\left(\frac{\partial^2}{\partial z^2} - q_0^2 + a^{-2}\mathrm{L}\right)^3 \Theta + (R_0 + a^{-4}\bar{R}^2)(q_0^2 - a^{-2}\mathrm{L})\,\Theta = 0; \\ &\Theta = \frac{\partial^2 \Theta}{\partial z^2} = \left(\frac{\partial^2}{\partial z^2} - q_0^2 + a^{-2}\mathrm{L}\right)\frac{\partial \Theta}{\partial z} = 0 \quad (z = \pm\tfrac{1}{2}), \end{aligned}\right\} \tag{5.4}$$

and an expansion for Θ as $a \to 0$ can proceed in the form

$$\Theta = g_0(Y, z) + a^{-2} g_1(Y, z) + a^{-4} g_2(Y, z) + \ldots, \tag{5.5}$$

where

$$\left\{\left(\frac{\partial^2}{\partial z^2} - q_0^2\right)^3 + R_0 q_0^2\right\} g_0 = 0; \quad g_0 = \frac{\partial^2 g_0}{\partial z^2} = \left(\frac{\partial^2}{\partial z^2} - q_0^2\right)\frac{\partial g_0}{\partial z} = 0 \quad (z = \pm\tfrac{1}{2}), \tag{5.6}$$

$$\left.\begin{aligned} &\left\{\left(\frac{\partial^2}{\partial z^2} - q_0^2\right)^3 + R_0 q_0^2\right\} g_1 = \mathrm{L}\left\{R_0 - 3\left(\frac{\partial^2}{\partial z^2} - q_0^2\right)^2\right\} g_0; \\ &g_1 = \frac{\partial^2 g_1}{\partial z^2} = 0, \quad \left(\frac{\partial^2}{\partial z^2} - q_0^2\right)\frac{\partial g_1}{\partial z} = -\mathrm{L}\frac{\partial g_0}{\partial z} \quad (z = \pm\tfrac{1}{2}), \end{aligned}\right\} \tag{5.7}$$

$$\left.\begin{aligned} &\left\{\left(\frac{\partial^2}{\partial z^2} - q_0^2\right)^3 + R_0 q_0^2\right\} g_2 = \mathrm{L}\left\{R_0 - 3\left(\frac{\partial^2}{\partial z^2} - q_0^2\right)^2\right\} g_1 - \left\{\bar{R}^2 q_0^2 + 3\mathrm{L}^2\left(\frac{\partial^2}{\partial z^2} - q_0^2\right)\right\} g_0; \\ &g_2 = \frac{\partial^2 g_2}{\partial z^2} = 0, \quad \left(\frac{\partial^2}{\partial z^2} - q_0^2\right)\frac{\partial g_2}{\partial z} = -\mathrm{L}\frac{\partial g_1}{\partial z} \quad (z = \pm\tfrac{1}{2}). \end{aligned}\right\} \tag{5.8}$$

Now the solutions of (5.6) and (5.7) can be written

$$g_0 = \bar{A}(Y)\,\bar{g}_0(z), \quad g_1 = -\mathrm{L}\bar{A}(Y)\,\bar{g}_1(z) + \bar{A}_1(Y)\,\bar{g}_0(z), \tag{5.9}$$

where $\bar{g}_0$ satisfies (5.6) but for the purpose of defining $\bar{g}_1$ may be construed as the solution associated with the neutral curve $R = R(q)$ of the generalized version of (5.6) in which $q_0 \to q$ and $R_0 \to R$, and then

$$\bar{g}_1 = \frac{1}{2q}\frac{\partial \bar{g}_0}{\partial q}\bigg|_{q=q_0}. \tag{5.10}$$

The existence of the solution for g_1 is equivalent to the fact that $\mathrm{d}R/\mathrm{d}q = 0$ at $R = R_0$; $\bar{A}_1$ is associated with a possible complementary solution for g_1 which will not affect the amplitude equation for $\bar{A}(Y)$. This equation is now determined from the solvability condition

$$\int_{-\frac{1}{2}}^{\frac{1}{2}} \chi_0\,\bar{g}\,\mathrm{d}z = \chi_1, \tag{5.11}$$

of the system for g_2. Here $\bar{g}$ is the adjoint of $\bar{g}_0$, satisfying

$$\left\{\left(\frac{\mathrm{d}^2}{\mathrm{d}z^2} - q_0^2\right)^3 + R_0 q_0^2\right\}\bar{g} = 0; \quad \bar{g} = \frac{\mathrm{d}\bar{g}}{\mathrm{d}z} = \left(\frac{\mathrm{d}^2}{\mathrm{d}z^2} - 2q_0^2\right)\frac{\mathrm{d}^2\bar{g}}{\mathrm{d}z^2} = 0 \quad (z = \pm\tfrac{1}{2}), \tag{5.12}$$

and from (5.8)

$$\chi_0 = \mathrm{L}^2\bar{A}\left\{3\left(\frac{\mathrm{d}^2}{\mathrm{d}z^2} - q_0^2\right)^2 - R_0\right\}\bar{g}_1 - \left\{3\mathrm{L}^2\left(\frac{\mathrm{d}^2}{\mathrm{d}z^2} - q_0^2\right) + \bar{R}^2 q_0^2\right\}\bar{A}\bar{g}_0, \tag{5.13}$$

$$\chi_1 = -\mathrm{L}^2\bar{A}\left[\frac{\mathrm{d}\bar{g}_1}{\mathrm{d}z}\frac{\mathrm{d}^2\bar{g}}{\mathrm{d}z^2}\right]_{-\frac{1}{2}}^{\frac{1}{2}}. \tag{5.14}$$

Thus

$$\left(\frac{\mathrm{d}^2}{\mathrm{d}Y^2}+\bar{q}\right)^2\bar{A}-c\bar{R}^2\bar{A}=0, \tag{5.15}$$

where

$$c = q_0^2\int_{-\frac{1}{2}}^{\frac{1}{2}}\bar{g}_0\bar{g}\,\mathrm{d}z\Big/\left\{\int_{-\frac{1}{2}}^{\frac{1}{2}}\bar{g}\left[\left(3\left(\frac{\mathrm{d}^2}{\mathrm{d}z^2}-q_0^2\right)^2-R_0\right)\bar{g}_1-3\left(\frac{\mathrm{d}^2}{\mathrm{d}z^2}-q_0^2\right)\bar{g}_0\right]\mathrm{d}z+\left[\frac{\mathrm{d}\bar{g}_1}{\mathrm{d}z}\frac{\mathrm{d}^2\bar{g}}{\mathrm{d}z^2}\right]_{-\frac{1}{2}}^{\frac{1}{2}}\right\}. \tag{5.16}$$

The even solutions of the linear systems for $\bar{g}_0$, $\bar{g}_1$ and $\bar{g}$ can be expressed in terms of hyperbolic functions whose coefficients are determined by application of the boundary conditions at $z=\frac{1}{2}$. Using this method the value of c is determined as 0.154 consistent with the value quoted by Kelly & Pal (1978) in their derivation of the Y-independent version of (5.15). In the stress-free case $\bar{g}_1$ can be taken as zero and, since $q_0=\pi/\sqrt{2}$, it is seen that (5.16) gives $c=\frac{1}{9}$, in agreement with (4.8). It should also be added that although higher-order corrections to R and q in (5.1) are envisaged, along with order a^{-1} and a^{-3} terms in (5.5) forced by the sidewall reaction (see below), their inclusion in the analysis does not influence the form of (5.15).

The core velocity and pressure fields corresponding to (5.5) are easily obtained from (3.2)–(3.6). At leading order it is found that

$$\left.\begin{aligned} U &\sim -\bar{A}q_0^{-1}\left(\frac{\mathrm{d}^2}{\mathrm{d}z^2}-q_0^2\right)\frac{\mathrm{d}\bar{g}_0}{\mathrm{d}z},\\ W &\sim -\bar{A}\left(\frac{\mathrm{d}^2}{\mathrm{d}z^2}-q_0^2\right)\bar{g}_0,\\ P &\sim -\bar{A}q_0^{-2}\left(\frac{\mathrm{d}^2}{\mathrm{d}z^2}-q_0^2\right)^2\frac{\mathrm{d}\bar{g}_0}{\mathrm{d}z}, \end{aligned}\right\} \tag{5.17}$$

and at order a^{-1}

$$V \sim -a^{-1}\frac{\mathrm{d}\bar{A}}{\mathrm{d}Y}q_0^{-2}\left(\frac{\mathrm{d}^2}{\mathrm{d}z^2}-q_0^2\right)\frac{\mathrm{d}\bar{g}_0}{\mathrm{d}z}, \tag{5.18}$$

so that in the core the cross-channel velocity component is an order-of-magnitude smaller than the other two components, confirming the two-dimensional nature of the motion. The values of $\bar{q}$ and $\bar{R}$ that determine the corrections to the critical wavenumber and Rayleigh number due to the presence of the lateral walls are found, as in the stress-free case, by matching the solution of (5.15) to an appropriate three-dimensional solution near each sidewall. If the same order-of-magnitude arguments apply then, for the region near $y=-a$,

$$(\Theta, U, V, W, P) \sim a^{-2}(\tilde{\theta}, \tilde{u}, \tilde{v}, \tilde{w}, \tilde{p})\,(\tilde{y}, z), \tag{5.19}$$

where $\tilde{\theta}(\tilde{y},z)$ satisfies the system (5.2) in which $y\to\tilde{y}$, $q\to q_0$ and $R\to R_0$, and $\tilde{y}=y+a$. Upon exclusion of solutions that are exponentially large as $\tilde{y}\to\infty$, it is found that

$$\tilde{\theta} = (\tilde{a}_0+\tilde{a}_1\tilde{y})\,\bar{g}_0+\tilde{a}_2(\tilde{y}^2\bar{g}_0-2\bar{g}_1)+\tilde{a}_3(\tilde{y}^3\bar{g}_0-6\tilde{y}\bar{g}_1)+\sum_{n=1}^{\infty}\tilde{b}_n\,\tilde{g}_n(z)\,\mathrm{e}^{-\alpha_n\tilde{y}}, \tag{5.20}$$

where $\tilde{g}_n$ and α_n are determined by solutions of the eigenvalue problem

$$\left(\left(\frac{\mathrm{d}^2}{\mathrm{d}z^2}+\omega\right)^3-R_0\omega\right)\tilde{g}=0;\quad \tilde{g}=\frac{\mathrm{d}^2\tilde{g}}{\mathrm{d}z^2}=\left(\frac{\mathrm{d}^2}{\mathrm{d}z^2}+\omega\right)\frac{\mathrm{d}\tilde{g}}{\mathrm{d}z}=0\quad(z=\pm\tfrac{1}{2}), \tag{5.21}$$

for which $\mathrm{Re}(\alpha_n) > 0$ and where $\omega = \alpha_n^2 - q_0^2$. It is expected that there are three infinite sets of these, although the first members of two of the sets correspond to $\alpha_n = 0$ and the special solutions associated with the further arbitrary constants $\tilde{a}_0, \ldots, \tilde{a}_3$.

Solutions for the other dependent variables associated with the temperature field (5.20) can easily be constructed and, in addition, there are solutions

$$(\tilde{u}, \tilde{v}) = \tilde{c}_n(-q_0, q_0^2(\alpha_0^2 + n^2\pi^2)^{-\frac{1}{2}})\, \mathrm{e}^{-(q_0^2+n^2\pi^2)^{\frac{1}{2}}\tilde{y}} \sin n\pi(z+\tfrac{1}{2}) \quad (n = 1, 2, \ldots), \tag{5.22}$$

which make no contribution to the temperature or vertical velocity fields. These, and another solution quadratic in z associated with $n = 0$, may be derived from the system (3.2)–(3.6) in which $y \to \tilde{y}$, $q \to q_0$ and $R \to R_0$. In all, this provides four infinite sets of coefficients to be fixed by the four boundary conditions (2.9) at $y = 0$ and matching with the core solution. Unfortunately the vertical eigenfunctions involved in (5.20) and (5.22) are not orthogonal and so a numerical method would be required to determine the values of the coefficients, although it can be assumed that only the even eigenfunctions in $\tilde{\theta}$ and the odd ones in $\tilde{u}$ and $\tilde{v}$ will be generated. If the solution is to match with that in the core as $\tilde{y} \to \infty$ it must be possible to specify $\tilde{a}_3$ and $\tilde{a}_2$ as in (4.16), so that although an infinite number of eigenfunctions will be required it appears that, in principle at least, $\tilde{a}_0$, $\tilde{a}_1$, $\tilde{b}_1$ and $\tilde{c}_2$ provide the necessary first set of four coefficients equivalent to the four conditions at $\tilde{y} = 0$. Any other scenario in which the core amplitude function does not satisfy the conditions (4.9) at $Y = \pm 1$ would imply an inconsistency in the neighbourhood of the sidewall.

The values of $\bar{q}$ and $\bar{R}$ at the critical point now follow from $\bar{q}_c$ and $\bar{R}_c$ of §4.1 and the transformation $9c\bar{R}^2 \to \bar{R}^2$. Thus at the onset of convection in a rigid channel

$$R_c \sim 1707.76 + 139.42a^{-4}, \quad q_c \sim 3.117 - 0.5127a^{-2} \quad \text{as} \quad a \to \infty. \tag{5.23}$$

These results are shown in figures 2 and 3.

6. Asymptotic results for the rigid channel: $a \to 0$

6.1. *Conducting sidewalls*

At small aspect ratios it must be anticipated that the conditions at the upper and lower boundaries do not greatly influence the onset of convection, suggesting that the stress-free scalings of the neutral curve given by (4.20) are still relevant. In the 'core' region $|Y| \leqslant 1$, $|z| < \frac{1}{2}$, which excludes the top and bottom of the channel,

$$\begin{bmatrix} \Theta \\ U \\ V \\ W \\ P \end{bmatrix} = \begin{bmatrix} a\Theta_1 \\ a^{-\frac{1}{2}}U_1 \\ V_1 \\ a^{-1}W_1 \\ a^{-2}P_1 \end{bmatrix} (Y, z) + \begin{bmatrix} a^2\Theta_2 \\ a^{\frac{1}{2}}U_2 \\ aV_2 \\ W_2 \\ a^{-1}P_2 \end{bmatrix} (Y, z) + \ldots, \tag{6.1}$$

and at leading order substitution into (3.2)–(3.6) gives

$$\frac{\partial^4\Theta_1}{\partial Y^4} - R_1\Theta_1 = 0; \quad \Theta_1 = \frac{\partial^2\Theta_1}{\partial Y^2} = 0 \quad (Y = \pm 1). \tag{6.2}$$

Thus $R_1 = m^4\pi^4/16$ and

$$\Theta_1 = \tilde{\Theta}(z) \sin\frac{m\pi}{2}(Y+1) \quad (m = 1, 2 \ldots), \tag{6.3}$$

where $\tilde{\Theta}$ is an arbitrary function of z to be determined. Corresponding solutions for the other variables are

$$\left.\begin{aligned} P_1 &= \tilde{P}(z), \quad U_1 = \tfrac{1}{2}q_1^{-\frac{1}{2}}(Y^2-1)\,\tilde{P}(z), \\ V_1 &= (\tfrac{1}{6}Y^3-\tfrac{1}{2}Y-\tfrac{1}{3})\,q_1\tilde{P}+\tfrac{1}{2}m\pi\left(\cos\frac{m\pi}{2}(Y+1)-1\right)\frac{\mathrm{d}\tilde{\Theta}}{\mathrm{d}z}, \\ W_1 &= \tfrac{1}{4}m^2\pi^2\tilde{\Theta}\sin\frac{m\pi}{2}(Y+1), \end{aligned}\right\} \tag{6.4}$$

where

$$\tilde{P} = \frac{3m\pi}{4q_1}((-1)^m-1)\frac{\mathrm{d}\tilde{\Theta}}{\mathrm{d}z}. \tag{6.5}$$

Note that for odd values of m the flux condition (2.10) implies that $\tilde{\Theta}(\frac{1}{2}) = \tilde{\Theta}(-\frac{1}{2})$ and for even values $\tilde{P} = 0$.

At second order Θ_2 is found to satisfy

$$\frac{\partial^4\Theta_2}{\partial Y^4}-R_1\Theta_2 = 2q_1\frac{\partial^2\Theta_1}{\partial Y^2}+R_2\Theta_1-\frac{\mathrm{d}P_1}{\mathrm{d}z}; \quad \Theta_2 = \frac{\partial^2\Theta_2}{\partial Y^2} = 0 \quad (Y=\pm 1). \tag{6.6}$$

This system has a solution only if

$$3q_1^{-1}((-1)^m-1)\frac{\mathrm{d}^2\tilde{\Theta}}{\mathrm{d}z^2}+(\tfrac{1}{2}m^2\pi^2q_1-R_2)\,\tilde{\Theta} = 0, \tag{6.7}$$

so that for even values of m a non-trivial solution requires $R_2 = \frac{1}{2}m^2\pi^2q_1$ in which case a minimum is achieved at $q_1 = 0$. For odd values of m, including the leading mode associated with $m = 1$, the boundary conditions for $\tilde{\Theta}$ are needed in order to solve (6.7).

At the base of the channel there is an adjustment in an end zone where

$$Z = (z+\tfrac{1}{2})/a = O(1),$$

but it is easily established that solutions for W and Θ of order a^{-1} and a respectively cannot depend on Z, in which case $\tilde{\Theta}(-\frac{1}{2}) = 0$. Similarly $\tilde{\Theta}(\frac{1}{2}) = 0$ and then, from (6.7), $\tilde{\Theta} = \sin n\pi(z+\frac{1}{2})$ for $n = 1, 2, \ldots$, where

$$R_2 = \tfrac{1}{2}\pi^2q_1(m^2+12n^2q_1^{-2}). \tag{6.8}$$

This coincides with the stress-free result (4.24) for $n = 1$ and so the asymptotic formulae (4.25) also apply to the rigid channel and are shown in figures 2 and 3. It may be verified that the end-zone solution where $Z = O(1)$ is actually generated by the core temperature gradient $\tilde{\Theta}'(-\frac{1}{2})$ so that locally $(\Theta, U, V, W) \sim (a^2\hat{\Theta}, a^{-\frac{1}{2}}\hat{U}, \hat{V}, \hat{W})$ (Y, Z).

6.2. *Insulating sidewalls*

Again the stress-free scalings (4.28) may be assumed and in the core

$$\begin{bmatrix}\Theta\\U\\V\\W\\P\end{bmatrix} = \begin{bmatrix}\Theta_1\\U_1\\aV_1\\W_1\\a^{-2}P_1\end{bmatrix}(Y,z)+\begin{bmatrix}a\Theta_2\\aU_2\\a^2V_2\\aW_2\\a^{-1}P_2\end{bmatrix}(Y,z)+\begin{bmatrix}a^2\Theta_3\\a^2U_3\\a^3V_3\\a^2W_3\\P_3\end{bmatrix}(Y,z)+\ldots, \tag{6.9}$$

as $a \to 0$. At leading order substitution into (3.2)–(3.6) gives

$$\left.\begin{aligned} &\Theta_1 = \tilde{\Theta}(z), \quad P_1 = \tilde{P}(z), \quad U_1 = \tfrac{1}{2}\bar{q}_1^{-\frac{1}{2}}(Y^2-1)\tilde{P}(z), \\ &V_1 = (\tfrac{1}{6}Y^3 - \tfrac{1}{2}Y - \tfrac{1}{3})\left(\bar{R}_1 \frac{\mathrm{d}\tilde{\Theta}}{\mathrm{d}z} - \frac{\mathrm{d}^2\tilde{P}}{\mathrm{d}z^2} + \bar{q}_1 \tilde{P}\right), \\ &W_1 = \tfrac{1}{2}(Y^2-1)\,\tilde{W}(z), \end{aligned}\right\} \tag{6.10}$$

where $\tilde{W} = (\mathrm{d}\tilde{P}/\mathrm{d}z) - \bar{R}_1 \tilde{\Theta}$ and the condition on V_1 at $Y = 1$ further implies $V_1 = 0$ and

$$\frac{\mathrm{d}^2\tilde{W}}{\mathrm{d}z^2} - \bar{q}_1(\tilde{W} + \bar{R}_1 \tilde{\Theta}) = 0. \tag{6.11}$$

The flux condition (2.10) implies that $\tilde{W}(\frac{1}{2}) = \tilde{W}(-\frac{1}{2})$. Similar solutions are obtained for Θ_2, W_2 etc. at second order, but at third order it is found that

$$\frac{\partial^2 \Theta_3}{\partial Y^2} = \bar{q}_1 \tilde{\Theta} - \frac{\mathrm{d}^2\tilde{\Theta}}{\mathrm{d}z^2} + \tfrac{1}{2}(1-Y^2)\,\tilde{W}, \tag{6.12}$$

so that the thermal boundary conditions at $Y = \pm 1$ can be satisfied only if

$$\frac{\mathrm{d}^2\tilde{\Theta}}{\mathrm{d}z^2} - \bar{q}_1 \tilde{\Theta} - \tfrac{1}{3}\tilde{W} = 0. \tag{6.13}$$

An assumption that $\tilde{\Theta}$ and $\tilde{W}$ remain non-zero as $z \to -\frac{1}{2}$ would imply a local solution near the base in which $(\Theta, W) \sim (\hat{\Theta}, \hat{W})(Y, Z)$ but it is easily shown that if $\hat{W}$ and $\hat{\Theta}$ vanish on $Z = 0$, they vanish for all Z. Hence $\tilde{W}(-\frac{1}{2}) = \tilde{\Theta}(-\frac{1}{2}) = 0$ and by a similar argument $\tilde{W}(\frac{1}{2}) = \tilde{\Theta}(\frac{1}{2}) = 0$. The coupled equations (6.11), (6.13) can now be solved to give

$$(\tilde{\Theta}, \tilde{W}) = \tilde{a}(1, -\bar{q}_1 \bar{R}_1/(n^2\pi^2 + \bar{q}_1)) \sin n\pi(z + \tfrac{1}{2}), \tag{6.14}$$

where

$$\bar{R}_1 = 3(\bar{q}_1 + 2n^2\pi^2 + n^4\pi^4 \bar{q}_1^{-1}) \quad (n = 1, 2, \ldots). \tag{6.15}$$

At the onset of convection for the vertical mode n, $\bar{q}_1 = n^2\pi^2$ and $\bar{R}_1 = 12n^2\pi^2$ so that the leading approximations to the critical Rayleigh number and wavenumber ($n = 1$) are given by the stress-free results (4.32).

7. Discussion

A two-dimensional Galerkin formulation of the Boussinesq equations in a rigid channel allows the cross-channel velocity to be taken into account and predicts values of the critical wavenumber and Rayleigh number in good agreement with asymptotic solutions for small and large aspect ratios. It seems likely that the numerical results are least accurate for these extreme cases where the end structures described in §§5 and 6 are presumably difficult to model accurately without specially selected trial functions. However, the results displayed in figures 2 and 3 provide an overall description of the onset of convection in a rigid channel for the complete range of aspect ratios. Even in wide channels the Galerkin procedure is sufficiently accurate to predict the three-dimensional motion near the sidewalls also characteristic of the idealized model with stress-free horizontal boundaries but omitted from the earlier discussion of the problem by Davies-Jones (1970). The flow reversal near the sidewalls is seen in numerical simulations of Rayleigh–Bénard convection in long, rigid boxes described by Oertel (1980). Results for convection in a nitrogen-filled box of length ten times and width four times its height clearly show the thin

regions of vertical flow reversal near the sidewalls. They arise at aspect ratios for which the critical wavelength exceeds its value for the corresponding infinite layer. For the rigid channel the maximum wavelength occurs when $a \approx 1.3$.

It is intended that the present theory will provide a basis for the investigation of weakly nonlinear effects in a long rigid box. Current theories of wavenumber selection at finite amplitudes (Cross *et al.* 1983) are restricted to two-dimensional models with stress-free horizontal boundaries, but an extension of the present theory would allow a realistic comparison with experimental work, which predicts that for low-Prandtl-number fluids the number of rolls decreases as the Rayleigh number is raised.

This work was carried out with the support of an SERC research grant.

Appendix. Galerkin integrals

The integrals appearing in (3.17)–(3.19) may be evaluated as follows, where $\bar{k} \leftrightarrow (\bar{m}, \bar{n})$, $k \leftrightarrow (m, n)$:

$$\int_{-a}^{a}\int_{-\frac{1}{2}}^{\frac{1}{2}} V_{\bar{k}}\bar{\nabla}^2\left(\frac{\partial^2}{\partial y^2}-q^2\right)V_k \,\mathrm{d}y\,\mathrm{d}z = 0 \quad (n \neq \bar{n}),$$

$$= \tfrac{1}{16}a^{-3}\mu_m^4 + aq^2(\delta_n - q^2) - \tfrac{1}{4}a^{-1}\delta_n\mu_m(2-\mu_m\coth\tfrac{1}{2}\mu_m)\coth\tfrac{1}{2}\mu_m \quad (n=\bar{n}, m=\bar{m}),$$

$$= 2a^{-1}\delta_n\frac{\mu_m^2\mu_{\bar{m}}^2}{\mu_m^4-\mu_{\bar{m}}^4}(\mu_{\bar{m}}\coth\tfrac{1}{2}\mu_{\bar{m}} - \mu_m\coth\tfrac{1}{2}\mu_m) \quad (n=\bar{n}, m\neq\bar{m}), \tag{A 1}$$

where $\delta_n = 2q^2 + 4n^2\pi^2$,

$$\int_{-a}^{a}\int_{-\frac{1}{2}}^{\frac{1}{2}} V_{\bar{k}}\bar{\nabla}^2\frac{\partial^2 W_k}{\partial y\,\partial z}\mathrm{d}y\,\mathrm{d}z = 32\pi^2 I_1(m,\bar{m},n,\bar{n}) \tag{A 2}$$

where

$$I_1(m,\bar{m},n,\bar{n}) = \frac{(-1)^{\bar{n}+m}\lambda_n^3\mu_{\bar{m}}^3\,\bar{n}(2m-1)(4\bar{n}^2\pi^2+\delta_m-q^2)\tanh\tfrac{1}{2}\lambda_n\coth\tfrac{1}{2}\mu_{\bar{m}}}{(\lambda_n^4-16\bar{n}^4\pi^4)(\mu_{\bar{m}}^4-(2m-1)^4\pi^4)} \tag{A 3}$$

and $\delta_m = 2q^2 + \frac{1}{4}a^{-2}(2m-1)^2\pi^2$,

$$\int_{-a}^{a}\int_{-\frac{1}{2}}^{\frac{1}{2}} W_{\bar{k}}\bar{\nabla}^2\left(\frac{\partial^2}{\partial z^2}-q^2\right)W_k \,\mathrm{d}y\,\mathrm{d}z = 0 \quad (m \neq \bar{m}),$$

$$= a\{\lambda_n^4 + q^2(\delta_m - q^2) - \delta_m\lambda_n(2-\lambda_n\tanh\tfrac{1}{2}\lambda_n)\tanh\tfrac{1}{2}\lambda_n\} \quad (m=\bar{m}, n=\bar{n}),$$

$$= 8a\delta_m\frac{\lambda_n^2\lambda_{\bar{n}}^2}{\lambda_n^4-\lambda_{\bar{n}}^4}(\lambda_{\bar{n}}\tanh\tfrac{1}{2}\lambda_{\bar{n}} - \lambda_n\tanh\tfrac{1}{2}\lambda_n) \quad (m=\bar{m}, n\neq\bar{n}), \tag{A 4}$$

$$\int_{-a}^{a}\int_{-\frac{1}{2}}^{\frac{1}{2}} W_{\bar{k}}\bar{\nabla}^2\frac{\partial^2 V_k}{\partial y\,\partial z}\mathrm{d}y\,\mathrm{d}z = 32\pi^2 I_1(\bar{m},m,\bar{n},n), \tag{A 5}$$

$$\int_{-a}^{a}\int_{-\frac{1}{2}}^{\frac{1}{2}} W_{\bar{k}}\Theta_k \,\mathrm{d}y\,\mathrm{d}z = 0 \quad (m \neq \bar{m})$$

$$= 4\pi a I_2(\bar{n}, n) \quad (m = \bar{m}) \tag{A 6}$$

where

$$I_2(\bar{n}, n) = \frac{(-1)^n\lambda_{\bar{n}}^2(1-2n)}{\lambda_{\bar{n}}^4-(2n-1)^4\pi^4}, \tag{A 7}$$

$$\int_{-a}^{a}\int_{-\frac{1}{2}}^{\frac{1}{2}} \Theta_{\bar{k}}\bar{\nabla}^2\Theta_k \,\mathrm{d}y\,\mathrm{d}z = -\tfrac{1}{2}a(\delta_m + (2n-1)^2\pi^2 - q^2) \quad (m=\bar{m}, n=\bar{n}),$$

$$= 0 \quad \text{(otherwise)}, \tag{A 8}$$

$$\int_{-a}^{a}\int_{-\frac{1}{2}}^{\frac{1}{2}} \Theta_{\bar{k}} W_k \,\mathrm{d}y\,\mathrm{d}z = 0 \quad (m \neq \bar{m}),$$

$$= 4\pi a I_2(n,\bar{n}) \quad (m=\bar{m}). \tag{A 9}$$

REFERENCES

Brown, S. N. & Stewartson, K. 1977 *Stud. Appl. Math.* **57**, 187.

Buhler, K., Kirchartz, K. R. & Oertel, H. 1979 *Acta Mech.* **31**, 155.

Catton, I. 1970 *Trans. ASME* C: *J. Heat Transfer* **92**, 186.

Chana, M. S. 1986 Thermal convection in channels and long boxes. Ph.D. thesis, The City University, London.

Cross, M. C., Daniels, P. G., Hohenberg, P. C. & Siggia, E. D. 1983 *J. Fluid Mech.* **127**, 155.

Daniels, P. G. 1977 *Proc. R. Soc. Lond.* A **358**, 173.

Daniels, P. G. 1978 *Mathematika* **25**, 216.

Daniels, P. G. & Ong, C. F. 1988 *Intl J. Heat Mass Transfer* (submitted).

Davies-Jones, R. P. 1970 *J. Fluid Mech.* **44**, 695.

Davis, S. H. 1967 *J. Fluid Mech.* **30**, 465.

Drazin, P. G. 1975 *Z. angew Math. Phys.* **26**, 239.

Harris, D. L. & Reid, W. H. 1958 *Astrophys. J. Suppl. Series* **3**, 429.

Kelly, R. E. & Pal, D. 1978 *J. Fluid Mech.* **86**, 433.

Kessler, R. 1987 *J. Fluid Mech.* **174**, 357.

Koschmieder, E. L. 1966 *Beitr. Phys. Atmos.* **39**, 1.

Koschmieder, E. L. & Pallas, S. G. 1974 *Intl J. Heat Mass Transfer* **17**, 991.

Luijkx, J. M. & Platten, J. K. 1981 *J. Non-Equilib. Thermodyn.* **6**, 141.

Newell, A. C. & Whitehead, J. A. 1969 *J. Fluid Mech.* **38**, 279.

Oertel, H. 1980 In *Natural Convection in Enclosures* (ed. K. E. Torrance & I. Catton), vol. 8, p. 11. ASME Heat Transf. Div.

Reid, W. H. & Harris, D. L. 1958 *Astrophys. J. Suppl. Series* **3**, 448.

Segel, L. A. 1969 *J. Fluid Mech.* **38**, 203.